Tunneling spectroscopy of quantum dots using submicrometer-diameter $Al_xGa_{1-x}As$-GaAs triple-barrier diodes

K. Nomoto, T. Suzuki, K. Taira, and I. Hase
Sony Corporation Research Center, 174 Fujitsuka-cho, Hodogaya-ku, Yokohama 240, Japan
(Received 18 June 1996; revised manuscript received 3 September 1996)

We have studied resonant tunneling (RT) through $Al_xGa_{1-x}As$-GaAs triple-barrier diodes with diameters between 0.2 and 10 μm. We have observed fine structures just above and below the RT threshold voltage V_{th} in the current-voltage curve of a submicrometer diode at $T=4$ K. With a diameter of 0.4–0.8 μm, the magnetic-field dependence and the sample dependence of the structure unambiguously show that (1) fine structures above V_{th} are caused by resonant tunneling (RT) through zero-dimensional (0D) states and coupled-0D states confined by the diode side-wall depletion region with a parabolic potential, and (2) fine structures below V_{th} are caused by RT through shallow-donor-bound states. Energy spacings of side-wall confined states and shallow-donor-bound energy are estimated to be 6.5 and 15–20 meV, respectively, which are consistent with a simple model. The tunneling current through the side-wall confined state is found to be proportional to the degeneracy of the 0D level confined by the parabolic potential. With a diameter of 0.2–0.3 μm, fine structures superimposed on the steplike structure were observed. We consider that those interplay between the 0D tunneling and a Coulomb blockade. The radius of a quantum dot estimated from a Coulomb staircase of 14 nm is in reasonable agreement with the extent of electron wavefunction in a quantum dot of 12 nm. [S0163-1829(97)09404-6]

I. INTRODUCTION

Significant properties of three-dimensionally confined systems, so-called quantum dots (QD), in semiconductor nanostructures are the quantization of the one-body energy and the large charging energy. To investigate such properties of a QD, tunneling spectroscopy has been used extensively. The structures used for spectroscopy are mainly laterally gated two-dimensional electron gas (2DEG)/depletion layer/2DEG(QD)/depletion layer/2DEG structure in an $Al_xGa_{1-x}As$/GaAs heterointerface[1] or small-area vertical $Al_xGa_{1-x}As$-GaAs double- (or triple-) barrier resonant tunneling diode (RTD) structures.[2–10] Especially in the latter structures, the difference between the Fermi level in the emitter and QD levels can be adjusted with a small change in the barrier height. This makes possible spectroscopy of a wide range of QD levels. Furthermore, the number of electrons in a QD of the latter structures can be changed starting from zero. This enables us to study the electronic properties of interacting few-electron systems.

Fine structures superimposed on main peaks have been observed in current-voltage (I-V) curves of submicrometer diameter RTD's. The main peaks are also observed in I-V curves of RTD's with diameters of more than several μm. These peaks are attributed to resonant tunneling through quasi-2D states confined vertically by a hetero barrier formed by crystal growth. The origins of the fine structures are understood to be a Coulomb staircase[5,6] and/or resonant tunneling through some sort of laterally confined state. There is a lively debate, however, about the origin of the laterally confining potential—surface depletion from the diode side wall,[2,3,5–7,9,10] impurity states,[8] and random potential fluctuations[10] are topics of discussion.

We have studied the tunneling spectroscopy of GaAs QD's using vertical $Al_xGa_{1-x}As$-GaAs triple-barrier RTD's (*coupled QD diodes*) with a diameter from 10 to 0.2 μm. We observed fine structures around the onset of 2D-2D resonant tunneling peaks in the I-V curves of diodes with a diameter between 0.8 and 0.2 μm. Previously, we reported an early result only about the fine structures in a positive bias with a 0.4-μm-diameter diode.[11] The result suggested that the fine structures were caused by 0D states in a QD and impurities. This paper is devoted to providing a more careful analysis of the origin of the fine structure in both a positive and a negative bias. The analysis takes not only the voltages of the fine structures but also the amplitude of their current into account. It is unambiguously found that the fine structures above and below the onset are respectively attributed to the tunneling through the zero-dimensionally (0D) quantized states laterally confined by the diode side-wall depletion layer and through shallow-donor bound states in the GaAs QD. In a positive bias, the fine structures are caused by tunneling through 0D levels in ''a single QD.'' On the other hand, in a negative bias, the fine structure is dominated by tunneling through 0D levels in ''a single QD and coupled QDs.'' We can determine that the side-wall confinement potential is a cylindrical parabolic potential in which the spacing of the quantized energy of an electron is 6.5 meV. The peak current of the fine structures is interestingly proportional to the degeneracy of the 0D level in the parabolic lateral potential. Although such peak-current quantization was reported by Tarucha *et al.* using $Al_xGa_{1-x}As$-GaAs double-barrier diodes that are laterally confined by a Ga focused-ion-beam implantation,[4] we do not know of any reports, except for this, about the observation of the peak-current quantization using a pillar of a RTD fabricated by an etching process. We can also estimate the bound energy of shallow-donor states to be 15–20 meV in the GaAs QD.

In I-V curves of smaller diodes with a diameter between

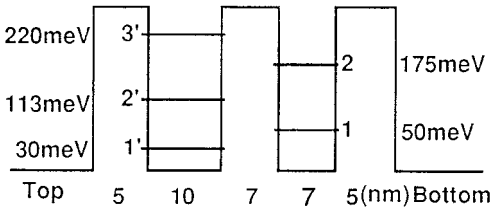

FIG. 1. Schematic band diagram of the $Al_xGa_{1-x}As$-GaAs triple-barrier structure investigated.

0.2 and 0.3 μm, we observed fine peak structures superimposed on steplike structures. We consider that these structures are related to the interplay between one-body energy quantization and the charging effects. The extent of an electron wave function in the GaAs QD estimated from the results of 0D quantized level spectroscopy is in reasonable agreement with the radius of conducting-channel area in the GaAs, estimated from the voltage width of the current plateau of the Coulomb staircase.

II. SAMPLE DESCRIPTION

The $Al_xGa_{1-x}As$-GaAs triple-barrier layer structure was grown by metalorganic chemical vapor deposition (MOCVD) on a (001)-oriented, 1×10^{18} cm^{-3} Si-doped GaAs substrate. The layer sequence was as follows: (i) 200-nm n^+ GaAs bottom contact layer ($n=3\times10^{18}$ cm^{-3}), (ii) 50-nm n^+ GaAs layer ($n=1\times10^{18}$ cm^{-3}), (iii) 5-nm GaAs spacer layer, (iv) 5-nm $Al_{0.3}Ga_{0.7}As$ bottom barrier, (v) 7-nm GaAs bottom well, (vi) 7-nm $Al_{0.3}Ga_{0.7}As$ middle barrier, (vii) 10-nm GaAs top well, (viii) 5-nm $Al_{0.3}Ga_{0.7}As$ top barrier, (ix) 5-nm GaAs spacer layer, (x) 50-nm n^+ GaAs layer ($n=1\times10^{18}$ cm^{-3}), and (xi) 100-nm n^+ GaAs top contact layer ($n=5\times10^{18}$ cm^{-3}). Silicon was used as the dopant. Layers (iii)–(ix) are all undoped. Diode pillars were defined using electron-beam or photolithography and $SiCl_4$/He mixture reactive ion etching. Ohmic contacts were made with alloyed AuGe/Ni/Au both at the top of the pillars and the back of the substrate. In the present experiment, we tried to fabricate diodes with diameters of 10–0.1 μm. However, Ohmic contacts could not be made to diodes with a diameter of 0.1 μm, possibly because the surface depletion layer at the diode side wall depleted the top GaAs contact channels. Therefore the depletion-layer width is estimated to be $\sim$0.05 μm. As a result, the minimum diameter of a diode successfully fabricated was 0.2 μm.

Figure 1 shows a schematic band diagram. The bottom energies in the 2D subband are obtained by calculating transmission probability at zero bias. The differences of the electron effective mass in the GaAs and $Al_xGa_{1-x}As$ layers and the nonparabolicity of electron energy dispersion in GaAs layers are taken into account.

III. RESULTS AND DISCUSSION

A. Coarse structure of the *I-V* characteristics

Figure 2 shows the overall *I-V* characteristics of the 0.4-μm-diameter diode. The voltage is applied with respect to the grounded substrate.

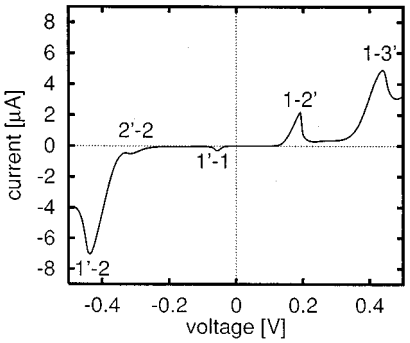

FIG. 2. Overall *I-V* characteristics measured at 4 K of a diode with a diameter of 0.4 μm. Quasi-2D tunneling is indicated by the band diagram in Fig. 1.

Here we discuss the coarse structure of the *I-V* characteristics. The main peaks, except that at -295 mV, are the resonant tunneling (RT) current peaks, which flow when the subband t' in the top well and the subband s in the bottom well are equal in energy. The spacings of voltage positions of the main peaks are identified as shown in Fig. 2 with the calculated subband spacing, using a voltage-energy conversion factor $\eta=e\Delta V/\Delta E$ of 2.2–3.1. The value of η is comparable to the value of 2.9 obtained by assuming a linear voltage drop in the undoped layers.

Using this value of η, we know that, at the voltage of -295 mV, the subband $2'$ is larger than the subband 2 by about 36 meV, which is similar to the energy of longitudinal-optical (LO) phonons in GaAs. From these results, we understand that the peak at -295 mV is due to the GaAs-like LO-phonon-emission-assisted $2'$-2 tunneling.

B. Tunneling current through 0D side-wall confined states and shallow donor states around 50 mV

Figure 3 shows the *I-V* characteristics at 4 K of the three different diodes with the same diameter of 0.4 μm. We observed fine structures above and below the RT threshold voltage of about 50 mV. As shown in Fig. 3, some *I-V* curves have fine structures only above the RT threshold voltage and others have them both above and below the RT threshold voltage.

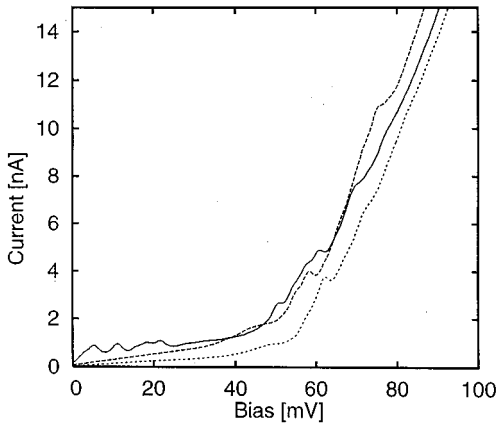

FIG. 3. *I-V* characteristics measured at 4 K of three triple-barrier diodes with the same diameter of 0.4 μm.

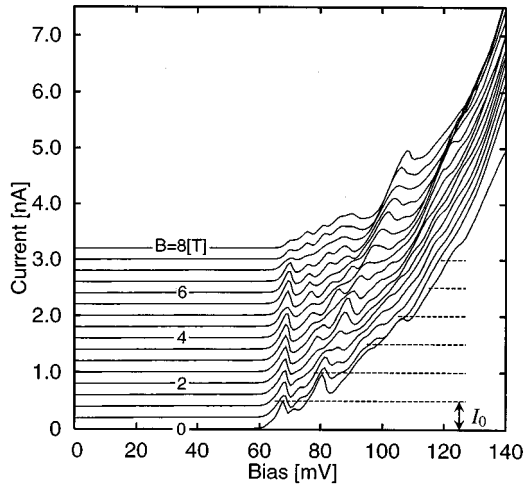

FIG. 4. The evolution of I-V characteristics at 4 K of a diode with a diameter of 0.4 μm, as the magnetic field applied parallel to the current flow is increased in steps of 0.5 T. Successive traces have been displaced upwards by 0.2 nA.

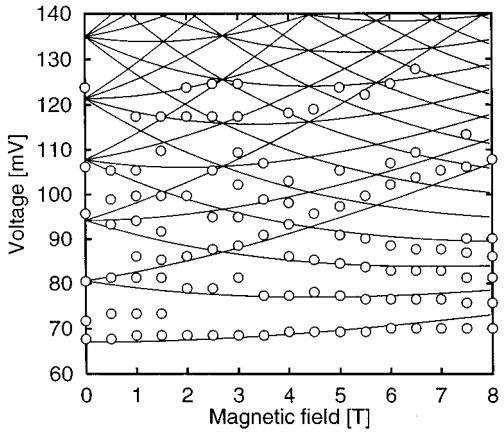

FIG. 5. Voltages at current peaks and shoulders as a function of magnetic field. Solid lines give the one-body energies calculated for a parabolic confining potential with Eq. (1) added to a constant offset using $\hbar\omega_0=6.5$ meV and the conversion factor of $\eta=2.2$.

First we will discuss the fine structures observed only above the RT threshold voltage. The qualitative structure did not depend on the sample. The fine structure was not clearly observed in diodes with a diameter of more than 1 μm. We measured the I-V characteristics under magnetic field B applied parallel to the current flow. As shown in Fig. 4, the results show a complicated shift of fine structures.

If the spacing of 0D quantized levels formed in a GaAs well is much larger than both the thermal energy k_BT and the spacing of energy levels in the emitter, fine structures can be observed in I-V characteristics when the Fermi level crosses the 0D quantized levels in the well.[12,13] When the well region is nearly pinched off, we assume that electrons are confined in the radial direction by side-wall depletion potential: $V(r_\perp)=m^*\omega_0^2 r_\perp^2/2$. If the magnetic field is applied parallel to the current flow, the eigenenergy in the radial direction becomes

$$E_{n,l}=(2n+|l|+1)\hbar(\omega_0^2+\omega_c^2/4)^{1/2}+l(\hbar\omega_c/2). \qquad (1)$$

Quantum numbers n and l are given by $n=0,1,2,\ldots$ and $l=0,\pm1,\pm2,...$, respectively. $\hbar\omega_0$ is the energy spacing for $B=0$, ω_c is the cyclotron frequency of the electron, eB/m^*, where m^* is the effective mass of an electron in a dot.

When the magnetic field is absent (i.e., $B=0$), Eq. (1) reduces to $E_{n,l}=(M+1)\hbar\omega_0$, where $M=2n+|l|$ and each energy has $(M+1)$-fold degeneracy for each spin. From Fig. 4, we find that for $B=0$, the amplitude of the Nth ($N=1,2,\ldots$) peak/shoulder from the lowest is approximated by NI_0, where $I_0=0.5$ nA is the lowest peak current. So we consider that the origin of such peak-current quantization is the degeneracy of QD levels. The small fine feature between the current peaks/shoulders specified by NI_0 is probably due to the overlap of the neighboring peaks. Such peak-current quantization was observed by Tarucha *et al.* using $Al_xGa_{1-x}As$-GaAs double-barrier diodes in which the lateral confining was imposed by Ga focused-ion-beam implantation.[4] To our knowledge, however, there is no observation of peak-current quantization using a RT-diode pillar laterally defined by the etching process.

A magnetic field lifts the degeneracy. In a strong magnetic field limit ($\omega_c \gg \omega_0$), the negative l level approaches the nth Landau level and the positive l level approaches the $(n+l)$th Landau level. As shown in Fig. 5, we obtain the best fitting between experimental data and calculated spectra using the value of $\hbar\omega_0=6.5$ meV. Even when $B\neq0$, we observe the amplitude of resonant tunneling, which is approximately proportional to the degeneracy of the 0D state, though the current is decreased as the magnetic field is increased.

Because the Fermi level at the GaAs side-wall surface is pinned at 0.7 eV below the conduction-band edge and the physical radius R of the diode is 0.2 μm, the Fermi level at the center of the diode pillar can be approximately calculated as $m^*\omega_0^2R^2/2-0.7$ eV$=0.04$ eV above the conduction-band edge in the GaAs well. If a few percent error of the diode radius is taken into account, the Fermi level is estimated to be around subband edge $1'$. This result is consistent with the fact that $1'$-1 resonant tunneling has been observed in our experiment. From these results, we confirm that the fine structures above 50 mV can be attributed to resonant tunneling through 0D quantized levels confined by the diode side-wall depletion layer. The deviation between the experimental data and the calculated curves in a high magnetic field is considered to be due to the nonparabolicity of the confinement potential and/or the shift of the levels in the bottom contact layer by the magnetic field.

Next we will discuss through what levels an electron tunnels. Because the fine structures are observed at the onset of the main peak of 1-$2'$ resonant tunneling, the fine structures seem to be produced by tunneling between 0D states in subband 1 and 0D states in subband $2'$. We conclude, however, that tunneling occurred between *3D states in the emitter and 0D states in subband 1′* for the following reasons.

(1) When we observe the tunneling current through the individual dot states, we see that the current begins to flow when the applied bias brings the emitter Fermi level, which should lie below subband $1'$ at zero bias, into resonance with subband $1'$. Based on this observation, the experimentally obtained RT thresholds of -30 and 50 mV can be repro-

duced by assuming that the Fermi level lies 16 meV below subband 1′. This value of the Fermi level is only 24 meV smaller than the value obtained by using Fermi-level pinning. (The difference can be explained by a 3-nm overestimation of diode diameter or nonparabolicity of the lateral confinement potential.) In this case, the fine structures are produced by resonant tunneling through 0D states in subband 1′. From the band diagram shown in Fig. 1 and using a conversion factor η of 2.9, resonant tunneling between subband 1 and subband 2′ occurs at a voltage of about 180 mV. In our experiment, however, fine structures were observed from 50 to 120 mV. The fine structures are not due to tunneling between subband 1 and subband 2′.

(2) It has been theoretically shown that tunneling from 3D emitter states into a 0D state in a QD (3D-0D tunneling) exhibits a peak when the Fermi level in the emitter and the 0D level are equal in energy.[14] Therefore fine structures caused by such tunneling can be mapped to energy levels of an electron in a QD.[12,13] However, the fine structure dominated by resonant tunneling between 0D states (0D-0D tunneling) cannot be so mapped.[15] We found that the fine structure can be mapped to the energy levels in a single QD as shown in Fig. 5 and that the peak current is proportional to the degeneracy of a single QD. Therefore we conclude that we observed tunneling through 0D states in a single QD. From the first reason, the 0D state should be in subband 1′.

For the emitter state, we consider that it behaves as a 3D system. The width of the surface depletion region in the emitter is found to be ~0.05 μm as discussed in Sec. II and therefore the diameter of the conducting core in the emitter of a 0.4-μm-diameter diode is ~0.3 μm. In such a case, the typical energy spacing in the emitter becomes several 0.1 meV. The energy spacing is too small to provide well-defined subbands at 4 K.

We have not observed 0D-0D tunneling under a positive bias. We consider the reason to be as follows. Under a positive bias, when the bias voltage (about 120 mV) brings the Fermi level in the emitter into resonance with subband 1, the lateral parabolic potential in the bottom GaAs well is screened and therefore flattened by accumulating electrons in the neighboring bottom spacer and the bottom GaAs well becomes a 2D system. Then the top GaAs well also becomes a 2D system due to screening by the accumulating electrons in the bottom GaAs well. As a result, above about 120 mV, the current flows by 2D-2D tunneling.

Next we will discuss fine structures at and below 50 mV. As shown in Fig. 3, they are observed for some samples, but not for other samples. The fine structures tended to disappear as the diameter of the diode gets smaller, as shown in Fig. 6. The fine structures are observed even for diodes with diameter of 10 μm and have strong sample dependence.

Based on the above, we consider that the fine structures arise from tunneling through *shallow-donor-bound states located in the GaAs top well*. If the width of the GaAs well is 5–10 nm, the ground-state energy of a shallow donor lies 20–15 meV below the bottom of the free 2D subband.[16] Using a conversion factor η of 2 to 3, the voltage at which tunneling through the shallow-donor states occurs should be 30–60 mV below the resonant threshold voltage $V_{\rm th}$. This is consistent with our experiment. The absence of the fine structures in I-V curves corresponds to the absence of (ionized) impurities in GaAs wells. The difference in the pattern of the fine structures would result from the difference of the distribution of impurities in GaAs wells.

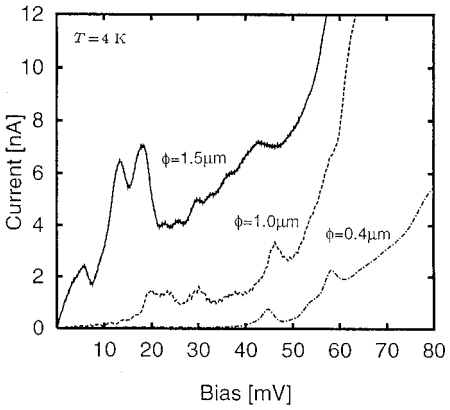

FIG. 6. Fine structures in I-V characteristics at 4 K of diodes with different diameters of 1.5 μm, 1.0 μm, and 0.4 μm.

Figure 7 shows the magnetic field dependence of I-V curves of a diode with a diameter of 6 μm. The quite complicated shift of the fine structures cannot be well fitted using Eq. (1). This is because the potential of an ionized impurity is closer to $1/r$ rather than to r^2. In our experiment, the Bohr radius of an electron (about 10 nm) is comparable with the cyclotron radius (about 26 nm at $B=1$ T). In such a case, it is impossible to derive the reasonably approximated analytic expression of the eigenenergy of an electron. Therefore, we have not obtained a good fit between the experimental data and the calculated impurity levels. In a system that corresponds to a hydrogen atom under a magnetic field, the classical motion of an electron shows chaotic behavior. Therefore, its quantum-mechanical nature attracts much attention in the context of quantum chaos.[17] Tunneling spectroscopy as in our experiments is expected to shed more light on this field.

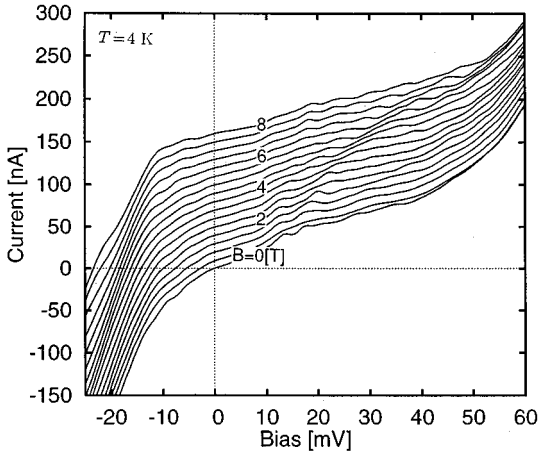

FIG. 7. The evolution of I-V characteristics at 4 K of a diode with a diameter of 6 μm, as the magnetic field applied to the current flow is increased in steps of 0.5 T. Successive traces have been displaced upwards by 10 nA.

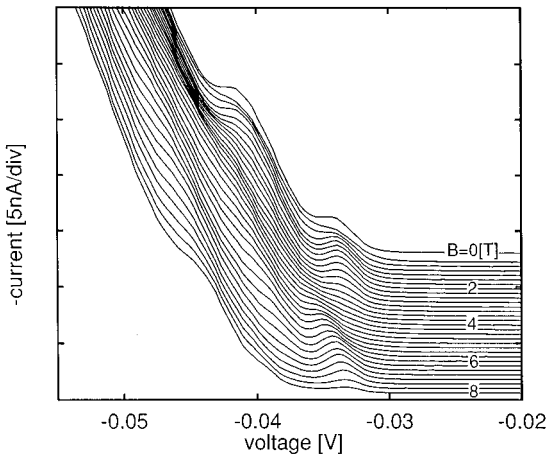

FIG. 8. The evolution of I-V characteristics at 4 K of a diode with a diameter of 0.4 μm, as the magnetic field applied to the current flow is increased in steps of 0.25 T. Successive traces have been displaced upwards by 0.4 nA.

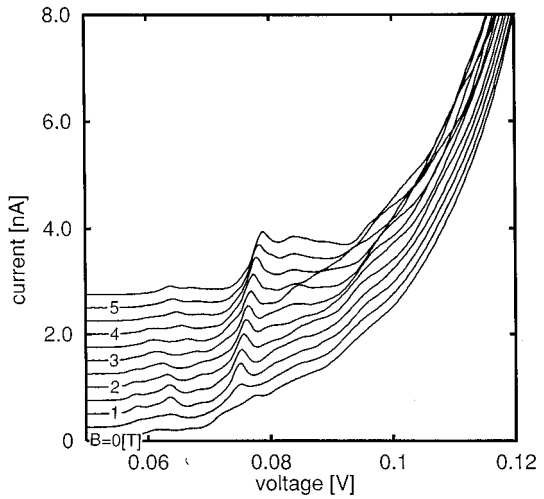

FIG. 9. The evolution of I-V characteristics at 4 K of a diode with a diameter of 0.3 μm, as the magnetic field applied to the current flow is increased in steps of 0.5 T. Successive traces have been displaced upwards by 0.4 nA.

C. 0D(-0D) tunneling around −30 mV

We observed two shoulder structures at −34 and −43 mV in the I-V curves for negative bias without a magnetic field, as shown in Fig. 8. Since this sample had no fine structures below the threshold voltage and all such samples exhibited the same pattern of fine structures, these fine structures were caused by the diode side-wall confinement but not by impurities. From energy-voltage conversion using the factor η=2.2 defined in Sec. III A, we can determine that the Fermi level in the emitter and the lowest level in the subband $1'$ are in alignment at −34 mV. At −34 mV, the lowest level in subband 1 is above and is not in resonance with the Fermi level in the emitter. Therefore the fine structure at −34 mV can be attributed to the tunneling between 3D states in the emitter and the 0D ground state in subband $1'$. Since we know that the spacing between 0D states in subband $1'$ is 6.5 meV, one may expect to observe tunneling through the first excited state in subband $1'$ at −48 mV (=−34 mV −6.5 meV$\times\eta/e$). However, at −43 mV, the bias brings the Fermi level in the emitter into resonance with the lowest level in subband 1. Therefore we observed a fine structure at −43 mV, which is not due to 0D tunneling only through subband $1'$, but to 0D-0D tunneling between an excited state in subband $1'$ and the ground state in subband 1. A perturbation of the translational invariance of the lateral confinement potential makes mode-mixing transitions possible. The fact that the fine structure cannot be mapped to 0D energy levels also supports 0D-0D tunneling mechanism. Teword *et al.* reported the observation of 0D-0D tunneling peaks on an overall $1'$-1 tunneling peak using submicrometer $Al_xGa_{1-x}As$-GaAs triple-barrier diodes.[9,10] However, we observed the fine structure only at the onset of $1'$-1 tunneling. We consider the reason as follows. Mode-mixing transitions cause the overlapping of many fine structures with narrow spacing in voltages. Furthermore the spacing of the 0D levels would be narrowed by the screening of the lateral potential caused by the accumulating electrons in the emitter next to the top GaAs well. If the voltage spacings are narrower than 1 mV, the overlapping cannot be resolved at 4 K and we observe 2D-2D tunneling without fine structures. We consider these are the reasons we observed only two fine structures between 0 to −43 mV and no fine structures above −50 mV. [On the other hand, at positive voltages from 0 to 120 mV, the Fermi level in the emitter is in resonance only with the subband $1'$ in the top GaAs well. Furthermore, since the GaAs top well is separated from the emitter by a thick (17 nm) depleted region, the lateral confining potential is hardly screened by electrons accumulated in the emitter. Therefore we can observe multiple fine structures caused by the tunneling through 0D states in subband $1'$.]

The amplitude of the fine structure at negative bias is modulated by the magnetic field as shown in Fig. 8. According to the transfer Hamiltonian formalism, the tunneling current is given by the product of density of states (DOS) in the emitter, and DOS in QD(s) and the transfer integral between the states in the emitter and the state in QD(s). Because energy levels are discrete in QD(s), the DOS in QD(s) does not change continuously and has a discrete value. The origin of the modulation is considered to be a change in DOS at the Fermi energy in the emitter or a change in the transfer integral due to some transitions like the spin-singlet–spin-triplet-like transition.[18]

D. Coulomb staircase observed in I-V characteristics of diodes with a diameter of 0.3–0.2 μm

Figure 9 shows the magnetic-field dependence of the fine structures in I-V characteristics observed at 4 K of a 0.3-μm-diameter diode. Magnetic fields were applied parallel to the current flow. The steplike structure was not affected by the magnetic fields, but was more clearly observed as the strength of the magnetic fields increased. On the other hand, the voltage position of the fine structure superimposed on the steplike structure shifted when the strength of the magnetic fields was increased. From these results, we consider that the steplike structure is a Coulomb staircase caused by charging of a QD and the fine structure was caused by RT through 0D quantized energy levels in a QD. From the results for a 0.4-μm-diameter diode, it has been found that the current begins

to flow when the applied bias brings the emitter Fermi level, which should lie below subband $1'$ at zero bias, into resonance with subband $1'$. Therefore, the current steps correspond to such increments of the number of electrons as $0\rightarrow1\rightarrow2\cdots$ in subband $1'$. At voltages higher than 100 mV, no steplike structure was observed. At such voltages, no more electrons may be accumulated in subband $1'$, because the bottom barrier height was lowered by the bias voltage and transmission probability through the barrier increased.

Since there were no electrons in subband 1 in the voltage region where the Coulomb blockade was observed, we approximate the device structure by a double tunneling junction system, where one junction whose capacitance is C_1 consists of an $Al_xGa_{1-x}As$ top barrier and the other junction whose capacitance is C_2 consists of an $Al_xGa_{1-x}As$ middle barrier, a GaAs bottom well and an $Al_xGa_{1-x}As$ bottom barrier. We assume that the capacitance C_i is given by $C_i=\varepsilon\pi r_{\rm cond}^2/d_i$, where ε is the permittivity of $Al_xGa_{1-x}As$, $r_{\rm cond}$ is the radius of conducting area and d_i is the width of the barrier. Since the barrier width is $d_1=5$ nm and $d_2=17$ nm, C_1 is larger than C_2. According to the orthodox theory of Coulomb blockade, the width of a current step of a Coulomb staircase is given by e/C_1, where C_1 is the larger junction capacitance.[19] The width of the current steps obtained from Fig. 9 is about 10 mV. Therefore, capacitance C_1 is estimated to be $C_1=e/10$ mV$=16$ aF. The radius $r_{\rm cond}$ of the conducting area is estimated to be $r_{\rm cond}=\sqrt{C_1d_1/(\varepsilon\pi)}=14$ nm. Alternately, the conducting area can be estimated from the lateral extent of the electron wave function, $r_{\rm wave}$, which is determined by the lateral confining potential in a QD. As we discussed in Sec. III B, the lateral confining potential of the QD is well approximated by a cylindrical dot with a parabolic potential: $V(r_\perp)=m\omega_0^2r_\perp^2/2$, where $\omega_0=(1/R)[(2\Phi)/m^*]^{1/2}$. Here Φ is the Fermi-level pinning of 0.7 eV at the diode side-wall surface and R is the physical radius of a diode. Here we define the lateral extent of the wave function, $r_{\rm wave}$, of the one-particle ground state as $r_{\rm wave}\equiv[\hbar/(m^*\omega_0)]^{1/2}=[\hbar R/(2m^*\Phi)^{1/2}]^{1/2}$. For a 0.3-$\mu$m-$(=2R)$ diameter diode, $r_{\rm wave}$ is estimated to be $\sim$12 nm. This value of 12 nm is in reasonable agreement with the radius of 14 nm estimated from the Coulomb staircase.

We observed a Coulomb staircase for 0.3-μm-diameter diodes, but we did not observe it for 0.4-μm-diameter diodes. The reason for this is not clearly understood. One possible explanation is the following. When a QD is nearly pinched off, the radii of the electron accumulating areas in QD's of 0.3-μm- and 0.4-μm-diameter diodes are not much different. The conducting area in the contact layer is, however, strongly influenced by the physical diameter of the diodes, because the width of the surface depletion region in the contact layer is only $\sim$50 nm, due to the high dopant concentration. For a 0.4-μm-diameter diode, the capacitance between the contact layer and the QD is not small enough to cause a Coulomb staircase, due to the large conducting area of the contact layer. In a 0.3-μm-diameter diode, the conducting area of the contact layer would be small enough for us to observe a Coulomb blockade at 4 K.

In I-V characteristics of another diode with a diameter of 0.2 μm, we observed considerably high resonant threshold voltages of -940 and 750 mV (see Fig. 10). A clear steplike structure was observed above the resonant threshold voltages. These current steps are considered to be caused by single-electron charging of quite small capacitors made not by $Al_xGa_{1-x}As$ layers but by fluctuations of the conducting path width.

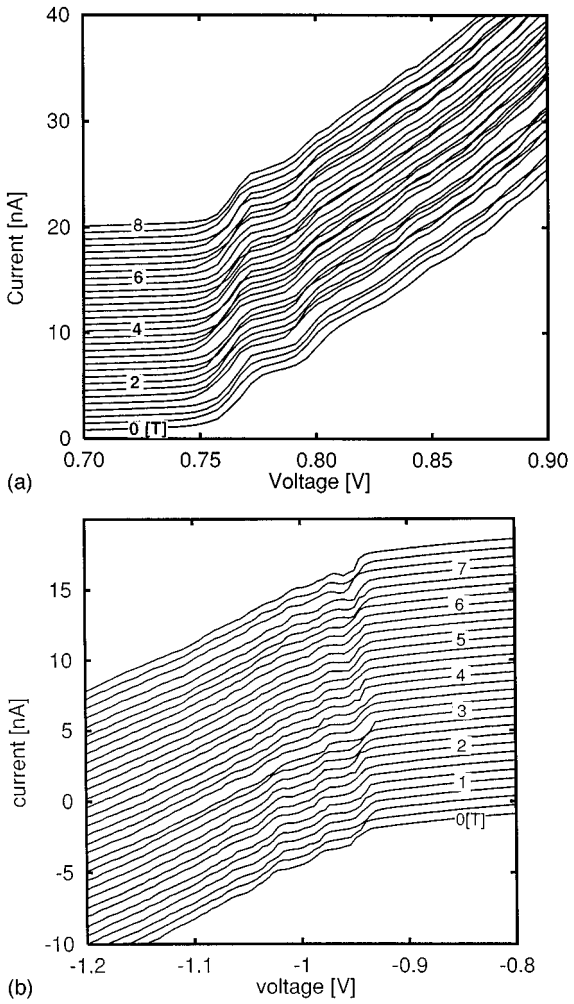

FIG. 10. The evolution of I-V characteristics at 4 K of a diode with a diameter of 0.2 μm for (a) positive bias and (b) negative bias, as the magnetic field applied to the current flow is increased in steps of 0.25 T. Successive traces have been displaced upwards.

IV. CONCLUSION

We have studied the low temperature I-V curves of submicrometer $Al_xGa_{1-x}As$-GaAs triple-barrier diodes. In the I-V curves of diodes with diameters of 0.4 μm, we observed fine structures above and below the resonant threshold voltage $V_{\rm th}$. Sample and magnetic field dependence of the voltage positions of the fine structures above $V_{\rm th}$ are well explained by the model in which an electron tunnels through 0D states in a single QD and coupled QD's laterally confined by a cylindrical-parabolic potential with $\hbar\omega_0=6.5$ mV. The amplitude of the fine structure is reasonably proportional to the degeneracy of 0D levels. These results confirm that the origin of the lateral confining potential is the diode side-wall depletion potential. The origin of the fine structure observed below the resonant threshold voltage is understood to be tun-

neling through the shallow donor states in GaAs wells. The bound energy is estimated to be 15–20 mV.

For 0.3- to 0.2-μm-diameter diodes, we observed a Coulomb staircase and tunneling through 0D states. The radius of the conducting channel area estimated from a Coulomb staircase of 14 nm is in reasonable agreement with the extent of wave function estimated from the magnetic field dependence of 0D levels of 12 nm.

ACKNOWLEDGMENTS

The authors would like to thank H. Kawai and S. Wada for MOCVD growth, and K. Funato for his help of magnetotunneling experiments. We are also grateful to T. Shimada for her technical assistance. This work was performed under the management of FED as a part of the MITI R&D program (Quantum Functional Devices Project) supported by NEDO.

[1] J. Weis, R. J. Hang, K. v. Klitzing, and K. Ploog, Phys. Rev. B **46**, 12 837 (1992); **24**, 4019 (1993); A. T. Jhonson, L. P. Kouwenhoven, W. de Jong, N. C. van der Vaart, C. J. P. M. Harmans, and C. T. Foxon, Phys. Rev. Lett. **69**, 1592 (1992).

[2] M. A. Reed, J. N. Randall, R. J. Aggarwal, R. J. Matyi, T. M. Moore, and A. E. Wetsel, Phys. Rev. Lett. **60**, 535 (1988).

[3] S. Tarucha, Y. Hirayama, T. Saku, and T. Kimura, Phys. Rev. B **41**, 5459 (1990).

[4] S. Tarucha, Y. Tokura, and Y. Hirayama, Phys. Rev. B **44**, 13 815 (1991).

[5] Bo Su, V. J. Goldman, and J. E. Chunningham, Superlattices Microstruct. **12**, 305 (1992).

[6] M. Tewordt, L. Martín-Moreno, J. T. Nicholls, M. Pepper, M. J. Kelly, V. J. Law, D. A. Ritchie, J. E. F. Frost, and G. A. C. Jones, Phys. Rev. B **45**, 14 407 (1992).

[7] M. Tewordt, D. A. Ritchie, R. T. Syme, M. J. Kelly, V. J. Law, R. Newbury, M. Pepper, J. E. F. Frost, G. A. C. Jones, and W. M. Stobbs, Appl. Phys. Lett. **59**, 1966 (1991).

[8] M. W. Dellow, P. H. Beton, C. J. G. M. Langerak, T. J. Foster, P. C. Main, L. Eaves, M. Henini, S. P. Beaumont, and C. D. W. Wilkinson, Phys. Rev. Lett. **68**, 1754 (1992).

[9] M. Tewordt, H. Asahi, V. J. Law, R. T. Syme, M. J. Kelly, D. A. Ritchie, A. Churchill, J. E. F. Frost, R. H. Hughes, and G. A. C. Jones, Appl. Phys. Lett. **60**, 595 (1992).

[10] M. Tewordt, R. J. F. Hughes, L. Martín-Moreno, J. T. Nicholls, H. Asahi, M. J. Kelly, V. J. Law, D. A. Ritchie, J. E. F. Frost, G. A. C. Jones, and M. Pepper, Phys. Rev. B **49**, 8071 (1994).

[11] K. Nomoto, T. Suzuki, K. Taira, and I. Hase, Jpn. J. Appl. Phys. **33**, L1142 (1994).

[12] G. W. Bryant, Phys. Rev. B **39**, 3145 (1989).

[13] G. W. Bryant, Phys. Rev. B **44**, 3782 (1991).

[14] H. C. Liu and G. C. Aers, J. Appl. Phys. **65**, 4908 (1989).

[15] G. W. Bryant, Phys. Rev. B **44**, 3064 (1991).

[16] G. Bastard, Phys. Rev. B **24**, 4714 (1981).

[17] P. Hawrylak and M. Grabowski, Phys. Rev. B **49**, 8174 (1994).

[18] M. Wagner, U. Merkt, and A. V. Chaplik, Phys. Rev. B **45**, 1951 (1992).

[19] J. R. Tucker, J. Appl. Phys. **72**, 4399 (1992).